IEEE Access
Multidisciplinary | Rapid Review | Open Access Journal

Received January 12, 2019, accepted February 5, 2019, date of publication February 15, 2019, date of current version March 5, 2019.

Digital Object Identifier 10.1109/ACCESS.2019.2899567

Rectangular Waveguide Differential Phase Shifter Based on Horizontal Ferrite Tiles: Accurate Model for Full-Band Operation

MOHAMED A. ABDELAAL, (Student Member, IEEE), SHOUKRY I. SHAMS, (Member, IEEE), AND AHMED A. KISHK, (Fellow, IEEE)
Electrical and Computer Engineering Department, Concordia University, Montreal, QC H3G 2W1, Canada
Corresponding author: Mohamed A. Abdelaal (mabdelaal@ieee.org)

ABSTRACT Phase shifters are one of the most important elements deployed in the antenna feeding structures. They are being used in several antenna systems for various applications. Moreover, they can be used in different microwave devices such as circulators and isolators. Furthermore, they are one of the commonly used components in circularly polarized antenna systems. They can be deployed using different techniques depending on the required electrical specifications and the power handling capability. Phase shifters with horizontal ferrite tiles have a higher power handling capability than the transistor based. Thus, this type of phase shifter was frequently visited in the literature. However, the previously presented models were either inaccurate or had a narrow validity range. Here, mathematical analysis and study have been performed for non-reciprocal differential phase shifters using two horizontal ferrite tiles based on waveguide technology. A new model is proposed along with the transcendental equation for the phase constant. The presented model is validated through comparison with various standard waveguides over the full band operation. Moreover, an experimental validation step is carried out, where the measured results have acceptable values.

INDEX TERMS Non-reciprocal components, ferrite, waveguide differential phase shifter, horizontal ferrite slabs, full-band phase shifter.

I. INTRODUCTION

Phase shifter plays an essential rule in many microwave communication applications. There are many examples of these applications such as electronic beam scanning systems [1]–[3] or circularly polarized antenna systems [4]–[6]. This can be performed by adding the phase shifter with any type of orthomode transducers to produce two orthogonal polarizations with 90° phase shift [7], [8]. The phase shifter can be implemented through many techniques such as delay lines [9], active element based phase shifters [10]–[13], and anisotropic element based phase shifters. Each technique is suitable for certain applications with some specific needs. Delay line phase shifters are very simple but they have a large size, and narrow bandwidth. Meanwhile, active phase shifters performance deteriorates significantly at high-frequency bands, especially those implemented with CMOS technology [14]–[16]. On the other hand, the ferrite material-based phase shifters show a leading edge over the other types as they have a high power handling capability in a compact size. Moreover, this type of phase shifters has a flat phase shift over the operating bandwidth. Due to this outstanding performance, the ferrite-based phase shifters have been deployed in many systems before [17]–[21].

Furthermore, Ferrite phase shifter is an important sub-component in other devices such as circulators, isolators, antenna beam scanning, switches, and duplexers [19], [22]–[26]. One example is the four-port differential phase shift circulator in which ferrite phase shifters are considered as a fundamental building block [27]–[32]. This importance of the ferrite-based phase shifters stimulates the research community to pay high attention to the development of such phase shifter, where many implementation technologies have been deployed. These technologies have many examples such as a waveguide, microstrip, stripline and substrate integrated waveguide [33]–[38]. Among all these

The associate editor coordinating the review of this manuscript and approving it for publication was Mohammad Tariqul Islam.

2169-3536 © 2019 IEEE. Translations and content mining are permitted for academic research only.
Personal use is also permitted, but republication/redistribution requires IEEE permission.
See http://www.ieee.org/publications_standards/publications/rights/index.html for more information.

implementation technologies, the rectangular waveguide has significant importance due to its power handling and compliance with standard systems.

Differential phase shifter based on ferrite material consists of two channels parallel to each other. Ferrite slabs in each waveguide channel are either having the same locations and magnetized in opposite directions, or same direction of magnetization and mirrored locations. This results in the required differential phase shift between both channels. It depends on the existence of natural planes of counter-rotating alternating magnetic fields with circular polarization on each side of its symmetry plane. The implementation technology of such shifter can be Substrate Integrated Waveguide as (SIW) as in [39] or Ridge Gap Waveguide (RGW) as in [40] and [41].

The traditional configuration of the ferrite differential phase shifter is based on deploying a vertical slab inside each channel. This solution has many problems and limitations, which will be discussed later in Section III. Changing the ferrite tiles geometry and allocation can solve these problems. For example, using two horizontal slabs instead of the vertical ones improves the thermal characteristic. This will be discussed in more details in Section II. The accurate solution of the two horizontal slabs is not visited thoroughly in the literature, and only the approximate solutions of the vertical slab are mentioned. The approximate solution considers only the filling factor of the ferrite material, regardless of the cross-section geometry and the orientation. In other words, the case of the vertical slab is thoroughly investigated. Meanwhile, other shapes utilize the same solution as an approximate expression, which deviates from the exact solution especially for filling factors above 1%. The filling factor is defined as the ratio between the ferrite and the channel cross-section areas. Hence, the traditional solutions are limited in terms of considering all configurations and geometries. This leaves a room for improvement to provide more accurate models for various differential phase shifter configurations.

This work presents an analysis and study of the waveguide differential phase shifter composed of two horizontal ferrite slabs in each channel. We propose an accurate model for calculating the phase constant. The transcendental equations are derived starting from Maxwell's equations and validated later by simulations and measurements. The proposed model has shown a maximum percentage error below 10%. An example of the differential phase shifter in Ka-band has been fabricated, where the measured results are in excellent agreement with the proposed model.

This paper is organized as follows; section II explains the different geometries of ferrite slabs inside each channel of the differential phase shifter. This is followed by a discussion of the traditional methods for designing such structures and their limitations in Section III. Section IV presents the proposed model of two horizontal ferrite slabs inside each channel. The validation of the introduced model is presented in Section V. Finally, the proposed model outcomes are summarized in Section VI.

II. FERRITE DIFFERENTIAL PHASE SHIFTER CONFIGURATION DESCRIPTION

The ferrite based differential phase shifter has different configurations based on the position and the cross-section shape of the ferrite material such as: rectangle, circle, square, or any other geometry. The commonly used ferrites have a rectangular cross-section due to the fabrication feasibility. The ferrite tiles with rectangular cross-section can be placed either in a vertical or in a horizontal orientation. This results in two common configurations: the vertical tile and the horizontal tile phase shifter. The configuration of the differential phase shifter consists of two channels parallel and adjacent to each other. One (or two) ferrite tile(s) with suitable magnetization is placed in each channel. The ferrite tiles in each waveguide are oppositely magnetized to produce the required differential phase shift between the two channels. To achieve the desired differential phase with the least filling factor (i.e., minimize the ratio of the ferrite cross-section to the channel cross-section), the ferrite tiles must be placed at the point of circular polarization inside the rectangular waveguide. In this way, there is no need to use a larger filling factor because it will be useless. The following equations determine the optimum position of the ferrite slab [33]:

$$\tan(k_c x) = \pm k_c/\beta_0 \tag{1}$$

where $k_c = \pi/a$, x is the location of the circular polarization point in the air filled guide, and β_0 is the propagation constant of the air filled guide, which is given by:

$$\beta_0 = \sqrt{k_0^2 - k_c^2} \tag{2}$$

In this paper, ferrite tiles of a rectangular cross-section are considered. This results in two distinct configurations for the differential phase shifters. The first case is the traditional one, in which a full height vertical ferrite tile is utilized. This case has a relatively high phase shift with high phase variations. The second case has less phase variations and it is recommended for wideband applications, in which two horizontal thin ferrite tiles are mounted on the top and bottom walls of the waveguide [33]. This case has a more flat response, and a wide operating band, however, it has a slightly lower phase shift compared with the vertical case. Fig. 1 shows the structure of a single channel according to the first and the second configurations. The max phase shift occurs when the ferrite is placed at a certain point at which two orthogonal magnetic field components are exactly equal to each other. This maximum phase shift point is frequency dependent. As a result, the narrow vertical tile can satisfy this condition for a narrower frequency band. On the other hand, the horizontal tile is able to cover wider range of frequencies with similar performance. This can explain the flat phase shift response of the horizontal tile compared with the vertical one. Moreover, the vertical tile configuration shown in Fig. 1(a) has two drawbacks [33]:

- Ferrite alignment difficulty: As the circular polarization point is a function of frequency, the wide frequency

TABLE 1. Comparison between differential phase shifters techniques.

Comparison Point	Vertical ferrite DPS [42]	Horizontal ferrite DPS (This work)
Implementation Technology	Rectangular waveguide	Rectangular waveguide
Operating B.W	34 GHz - 40 GHz	Full-band for any standard waveguide
Bandwidth Percentage	16.2%	40%
Maximum Phase Variation Over B.W	20°	15°

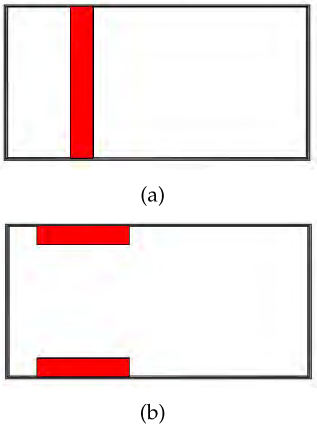

FIGURE 1. Each channel of the ferrite differential phase shifter deploying. (a) One vertical tile. (b) Two horizontal tiles.

variation because the optimum point to be outside the slab width. Therefore, the ferrite will not be fully enabled.

- The vertical orientation of the ferrite slab leads to a small contact area between the ferrite and the metal, which reduces the heat transfer and increases the temperature significantly under high power conditions.

A comparison between the vertical and the horizontal ferrite slabs Differential Phase Shifter (DPS) is presented in Table 1.

It is worth to mention that selecting the right ferrite material and applying the suitable magnetic bias is a critical step in building phase shifters. The ferrite selection criteria are illustrated in details in Appendix VI. It is essential to understand this process deeply before going through either the traditional design methodologies or the proposed work as the same guidelines have to be considered in all cases.

III. TRADITIONAL DESIGN METHODOLOGY LIMITATIONS

In this section, the traditional solution of the differential phase shifter problem is discussed, where the current limitations are highlighted. The basic configuration for the differential phase shifter is considered, in which the ferrite slab has a vertical orientation as shown in Fig. 1(a). The vertical ferrite slab is centered at the point of circular polarization inside the rectangular waveguide. In order to find the differential phase occurs due to the existence of the ferrite slab the phase propagation constant β has to be evaluated. The solution in this case is simple and straightforward. However, the vertical tile phase shifter has many limitations compared with the horizontal orientation in terms of both the electrical and thermal characteristics as mentioned before.

The transcendental equation is obtained in the literature in the case of the vertical tile [29], [33]. Afterward, these provided formulas have been simplified to introduce an approximate expression for the phase shift [33].

$$\Delta\beta = 2k_c \frac{\kappa}{\mu} \frac{\Delta S}{S} \sin(2k_c m) \tag{3}$$

where κ and μ are the elements of the permeability tensor of the ferrite material. Moreover, $\frac{\Delta S}{S}$ represents the filling factor that is equivalent to the cross-section area of the ferrite divided by the cross-section area of the waveguide. Although this expression has been extracted for the vertical tile case, it is utilized in other ferrite shapes as long as the filling factor is below 1% (i.e. $\frac{\Delta S}{S} < 0.01$).

In conclusion, although the case of two horizontal slabs is significant due to its advantages compared with the vertical case as explained before, it has not been well investigated in the literature. The approximate expression has an acceptable percentage error for small filling factor ($\frac{\Delta S}{S}$), but these small filling factors are not practical since the differential phase shifter in this case needs a long length to accomplish the desired phase shift value. In order to reduce the length of the ferrite slab, the high filling factor is needed. Accordingly, we are proposing an accurate model to solve the differential phase of the horizontal slabs case that is valid for large values of the filling factor, with a maximum error below 10% in the following section.

IV. PROPOSED MODEL

As a first step, we propose to model the horizontal tile differential phase shifter with an equivalent waveguide, where the horizontal tiles and the intermediate air filling will be replaced by a single effective homogeneous medium. The equivalent slab has the same cross-section area, but it has an effective permeability and an effective dielectric constant. These two parameters depend on the filling factor of the ferrite material. This equivalent model is expected to achieve accurate results only if the ferrite filling is distributed along the region. This case will be entitled as the homogeneous case, which is not practical as the possible configuration is to attach the ferrite material to the top and the bottom walls. A second step is performed to reach an accurate model that can be applied to the realistic case, where the ferrite slabs exist at the top and the bottom wall. In this step, the physical width of the ferrite slab is replaced by an effective one to take into consideration the discontinuity effect. In the following part, these two steps are discussed in detail starting from the first principles to obtain the required model.

A. HOMOGENEOUS CASE TRANSCENDENTAL EQUATION

The original structure of the phase shifter is shown in Fig. 2(a), while the proposed equivalent model is shown in Fig. 2(b). The structure of the equivalent model consists of three regions, where region 1 and region 3 are air-filled, while region 2 represents the effective material of the ferrite tiles. The idea used for region 2 which is shown in equations 4, 5, and 6 is to define the effective parameters through calculating the filling ratio between the ferrite and the air. Thus, it can be considered as averaging the values of μ, κ, and ϵ. Later, the correction factor is added to these equations to decrease the error. The elements of permeability tensor and the permittivity of region 1 and 3 are $\mu_{(1),(3)} = \mu_0$, $\kappa_{(1),(3)} = 0$, $\epsilon_{(1),(3)} = \epsilon_0$, respectively. On the other hand, both the permeability and the permittivity in region 2 are assumed to be:

$$\mu_{eff\,(2)} = \frac{h_f}{b}(\mu_0\left[1 + \frac{f_0 f_m}{f_0^2 - f^2}\right]) + (1 - \frac{h_f}{b})\mu_0 \quad (4)$$

$$\kappa_{eff\,(2)} = \frac{h_f}{b}\mu_0\left[\frac{f f_m}{f_0^2 - f^2}\right] \quad (5)$$

$$\epsilon_{eff\,(2)} = \frac{h_f}{b}\epsilon_r\epsilon_0 + (1 - \frac{h_f}{b})\epsilon_0 \quad (6)$$

Hence, the permeability tensor $[\mu_{eff\,(2)}]$ for the $\hat{y}$ bias will be:

$$[\mu_{eff\,(2)}] = \begin{bmatrix} \mu_{eff\,(2)} & 0 & -j\kappa_{eff\,(2)} \\ 0 & \mu_0 & 0 \\ j\kappa_{eff\,(2)} & 0 & \mu_{eff\,(2)} \end{bmatrix} \quad (7)$$

The phase propagation constant β of the equivalent model will be obtained from Maxwell equations that can be written in the case of source free as:

$$\nabla \times \vec{E} = -j\omega\vec{B} \quad (8)$$

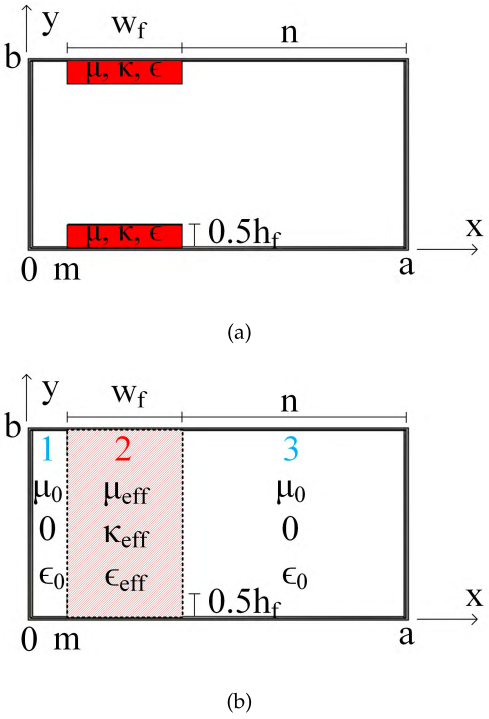

FIGURE 2. Each channel of the ferrite differential phase shifter. (a) Actual structure. (b) Effective model.

$$\nabla \times \vec{H} = j\omega\vec{D} \quad (9)$$

For linear isotropic mediums:

$$\nabla \times \vec{E} = -j\omega\mu\vec{H} \quad (10)$$

$$\nabla \times \vec{H} = j\omega\epsilon\vec{E} \quad (11)$$

As the ferrite materials are anisotropic materials, the magnetic flux density and the magnetic field can be related to each other by the following relation in region 2:

$$\vec{B} = [\mu_{eff}]\vec{H} \quad (12)$$

Assuming $\vec{E}$ and $\vec{H}$ are:

$$\vec{E}(x, y, z) = [\vec{e}(x, y) + \hat{z}e_z(x, y)]e^{-j\beta z} \quad (13)$$

$$\vec{H}(x, y, z) = [\vec{h}(x, y) + \hat{z}h_z(x, y)]e^{-j\beta z} \quad (14)$$

Enforcing the boundary conditions in the three regions a resultant transcendental equation for the propagation constant β can be derived.

By solving Maxwell's equations based on $\vec{E}$ and $\vec{H}$ in (13) and (14), and if the propagating mode is TE_{10}, the equations are reduced to:

$$j\beta e_y = -j\omega(\mu_{eff})_{(2)}h_x - j\kappa_{eff\,(2)}h_z) \quad (15)$$

$$\frac{\partial e_y}{\partial x} = -j\omega(j\kappa_{eff\,(2)}h_x + \mu_{eff\,(2)}h_z) \quad (16)$$

$$j\omega\epsilon_{eff\,(2)}e_y = -j\beta h_x - \frac{\partial h_z}{\partial x} \quad (17)$$

Solving (15) and (16) to find h_x and h_z

$$h_x = -\frac{\beta e_y}{\omega\mu_f} - \frac{\kappa_{eff\,(2)}}{\omega\mu_f\mu_{eff\,(2)}}\frac{\partial e_y}{\partial x} \quad (18)$$

$$h_z = \frac{j\kappa_{eff(2)}\beta e_y}{\omega\mu_f\mu_{eff(2)}} + \frac{j}{\omega\mu_f}\frac{\partial e_y}{\partial x} \tag{19}$$

where here the factor μ_f is defined by

$$\mu_f = \frac{\mu_{eff(2)}^2 - \kappa_{eff(2)}^2}{\mu_{eff(2)}} \tag{20}$$

Substitute by (18), (19), and (20) in (17) to find the wave equation e_y:

$$\begin{aligned} j\omega\epsilon_{eff(2)}e_y = &(\frac{j\beta}{\omega\mu_{eff(2)}\mu_f})(\mu_{eff(2)}\beta e_y + \kappa_{eff(2)}\frac{\partial e_y}{\partial x}) \\ &-(\frac{j}{\omega\mu_{eff(2)}\mu_f})(\kappa_{eff(2)}\beta\frac{\partial e_y}{\partial x} + \mu_{eff(2)}\frac{\partial^2 e_y}{\partial x^2}) \end{aligned} \tag{21}$$

Obtaining the corresponding results for region 1 and 3:

$$(\frac{\partial^2}{\partial x^2} + k_f^2)e_y = 0 \tag{22}$$

where k_f is the cutoff wave number for the ferrite and it is related to β by:

$$k_f^2 = \omega^2\mu_f^2\epsilon_{eff(2)} - \beta^2 \tag{23}$$

k_a is the cutoff wave number of the air regions and it is related to β by:

$$k_a^2 = k_0^2 - \beta^2 \tag{24}$$

h_x and h_z in the air region are given by:

$$h_x = -\frac{\beta}{\omega\mu_0}e_y \tag{25}$$

$$h_z = \frac{j}{\omega\mu_0}\frac{\partial e_y}{\partial x} \tag{26}$$

The solution of e_y inside the waveguide that can satisfy the boundary conditions for the three regions:

$$e_y = \begin{cases} C_1\sin k_a x, & \text{for } 0 < x < m \\ C_2\sin k_f(x-m) & \\ \quad +C_3\sin k_f(m+w_f-x), & \text{for } m < n < m+w_f \\ C_4\sin k_a(a-x), & \text{for } m+w_f < n < a \end{cases} \tag{27}$$

Using (26) and (27) to get h_z and then matching e_y with h_z at $x = m, x = m + w_f = a - n$ results in four equations for the constants C_1, C_2, C_3, and C_3:

$$C_1\sin(k_a m) = C_3\sin(k_f w_f) \tag{28}$$

$$C_2\sin(k_f w_f) = C_4\sin(k_a n) \tag{29}$$

$$\begin{aligned} \frac{C_1 k_a}{\mu_0}\cos k_a m = &\frac{C_2 k_f}{\mu_f}\frac{C_3}{\mu_{eff(2)}\mu_f}(\kappa_{eff(2)}\beta\sin k_f w_f \\ &-\mu_{eff(2)}k_f\cos k_f w_f) \end{aligned} \tag{30}$$

$$\begin{aligned} \frac{C_4 k_a}{\mu_0}\cos k_a n = &\frac{C_3 k_f}{\mu_f} - \frac{C_2}{\mu_{eff(2)}\mu_f}(\kappa_{eff(2)}\beta\sin k_f w_f \\ &+\mu_{eff(2)}k_f\cos k_f w_f) \end{aligned} \tag{31}$$

By solving (28) and (29) and substituting in (30) and (30), then eliminating all the constants results in a transcendental equation for the propagation constant β as:

$$\begin{aligned} &(\frac{k_f}{\mu_f})^2 + (\frac{\kappa_{eff(2)}\beta}{\mu_{eff(2)}\mu_f})^2 \\ &\quad -\frac{k_a}{\tan k_a m}(\frac{k_f}{\mu_0\mu_f\tan k_f w_f} + \frac{\kappa_{eff(2)}\beta}{\mu_0\mu_{eff(2)}\mu_f}) \\ &\quad -(\frac{k_a}{\mu_0})^2\frac{1}{\tan k_a m\tan k_a n} \\ &\quad -\frac{k_a}{\tan k_a n}(\frac{k_f}{\mu_0\mu_f\tan k_f w_f} - \frac{\kappa_{eff(2)}\beta}{\mu_0\mu_{eff(2)}\mu_f}) = 0 \end{aligned} \tag{32}$$

In this case, the total area of the ferrite material ($\Delta S = w_f \times b$) is uniformly distributed over the waveguide cross-section area ($S = a \times b$) in such way the medium in this area is a homogeneous medium. As the number of the ferrite slabs number increases and their thickness decrease but with the same filling factor, the medium can be considered homogeneous. The ideal case is represented by the proposed model so far to have an infinite number of horizontal slabs with almost zero thickness. To prove this claim, different configurations are investigated and shown in Figs 3(a), 3(b). In these configurations, the ferrite material is distributed over four and eight strips, respectively. The phase shift is extracted numerically and compared with the realistic case (Two slabs) and the homogeneous model in Fig. 3(c). This figure shows that as long as the ferrite is distributed more, the phase shift response is getting closer to the proposed homogeneous model.

B. INHOMOGENEOUS CASE ADJUSTMENT

In this case, the two distinct ferrite horizontal slabs are considered, the ferrite slab total area is not uniformly distributed over the cross-section area $w_f \times b$, that means the ferrite medium here is inhomogeneous medium. Due to the sudden discontinuities between the ferrite and the air. Some adjustment must be performed for the proposed model. Fringed fields above the ferrite slab lead to an effective height slightly larger than the physical height. This can be represented mathematically with a correction factor CF. Hence, h_f in Equations (4), (5), and (6) will be replaced with h_f' as

$$h_f' = CF \times h_f \tag{33}$$

Figure 7 shows the variation of the phase constant versus frequency for the right hand circularly polarized, the left hand circularly polarized components and the difference.
where CF is a correction factor that represents the in-homogeneity of the ferrite distribution. The empirical expression that represents this correction factor is extracted through comparison with the extracted results numerically over several standard rectangular waveguides. Many parametric sweeps are performed such as the ferrite slab dimensions and parameters. Then, the final CF is obtained numerically. Furthermore, if the ferrite filling factor is less

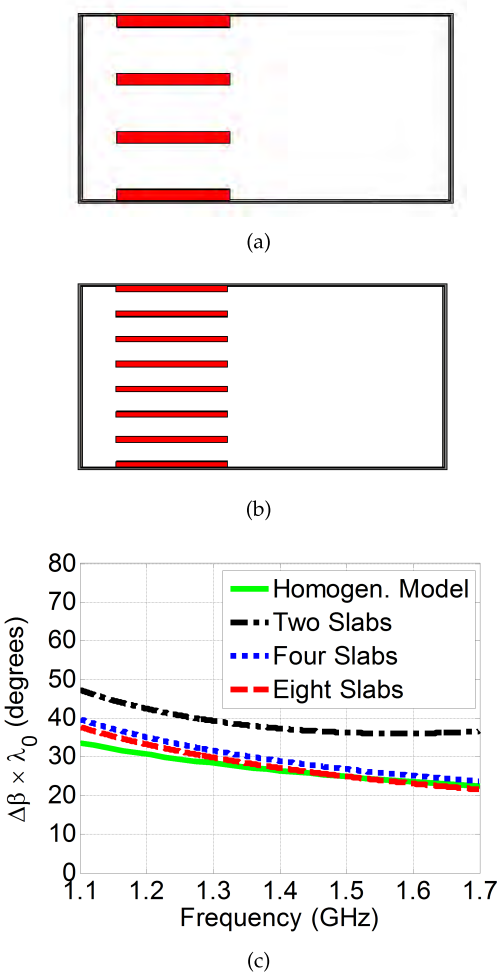

FIGURE 3. Ferrite material distribution. (a) Four tiles. (b) Eight tiles. (c) Simulation results comparison (WR-650, $4\pi M_s = 300$ G, $H_0 = 120$ Oe, $\frac{\Delta S}{S} = 0.075$).

TABLE 2. Correction Factor Equation Constants.

Parameter	Value	Parameter	Value
a_1	0.16	b_1	1.18
a_2	0.90	b_2	0.21
a_3	7.10	b_3	0.11
a_4	1.08		

than 7.5% ($\frac{\Delta S}{S} \leq 0.075$) with an aspect ratio between 5 and 9, the CF is valid for any waveguide dimension and operating frequency. The correction factor is represented by the following equation:

$$CF = F_1 \times F_2 \tag{34}$$

where F_1 and F_2 can be defined by the following equations that have the constants shown in Table 2.

$$F_1 = a_1 \times \arctan(a_2 \times 100 \times \frac{\Delta S}{S} - a_3) + a_4 \tag{35}$$

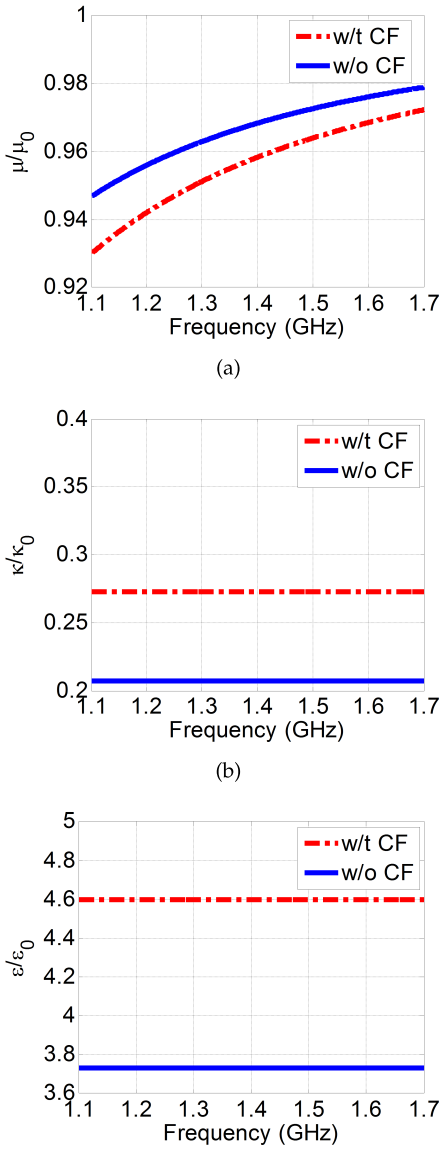

FIGURE 4. The effective model parameters in the case of WR-650 ($4\pi M_s = 300$ G, $H_0 = 120$ Oe, $\frac{\Delta S}{S} = 0.075$, $Fr_{asr} = 7$). (a) $\frac{\mu}{\mu_0}$. (b) $\frac{\kappa}{\kappa_0}$. (c) $\frac{\epsilon}{\epsilon_0}$.

$$F_2 = b_1 \times \sin(b_2 \times Fr_{asr}) + b_3 \tag{36}$$

where Fr_{asr} is the aspect ratio of each ferrite tile cross-section area that is given by the following equation using the parameters shown in Fig. 2.

$$Fr_{asr} = W_f / h_f \tag{37}$$

Based on equation (33), the correction factor represents the essential modification in the ferrite slab height for the model to obtain accurate values for the phase shift. As the model is based on a physical insight and the correction factor compensates only for the inhomogeneous distribution of the ferrite material, it is expected to have a constant

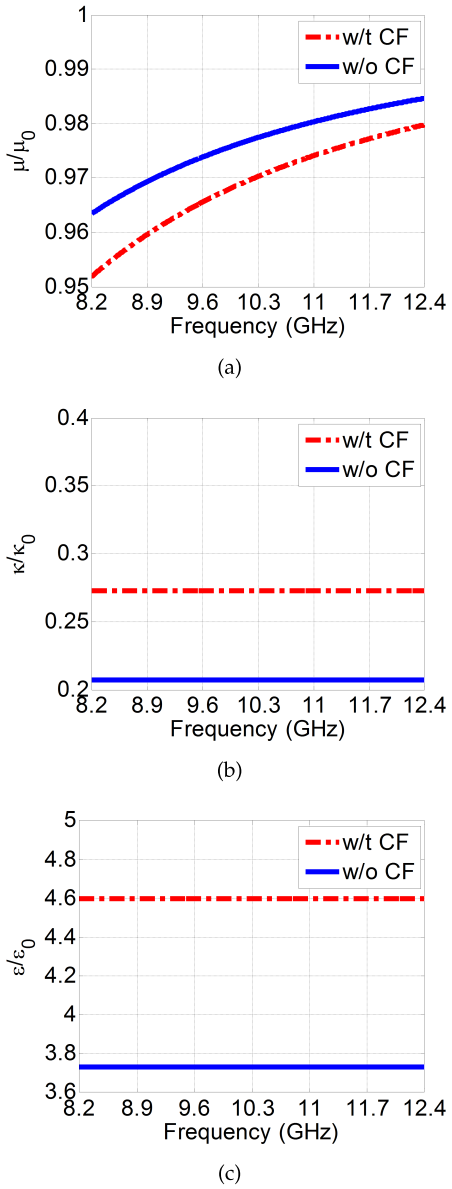

FIGURE 5. The effective model parameters in the case of WR-90 ($4\pi M_s = 1880$ G, $H_0 = 752$ Oe, $\frac{\Delta S}{S} = 0.075$, $Fr_{asr} = 7$). (a) $\frac{\mu}{\mu_0}$. (b) $\frac{\kappa}{\kappa_0}$. (c) $\frac{\epsilon}{\epsilon_0}$.

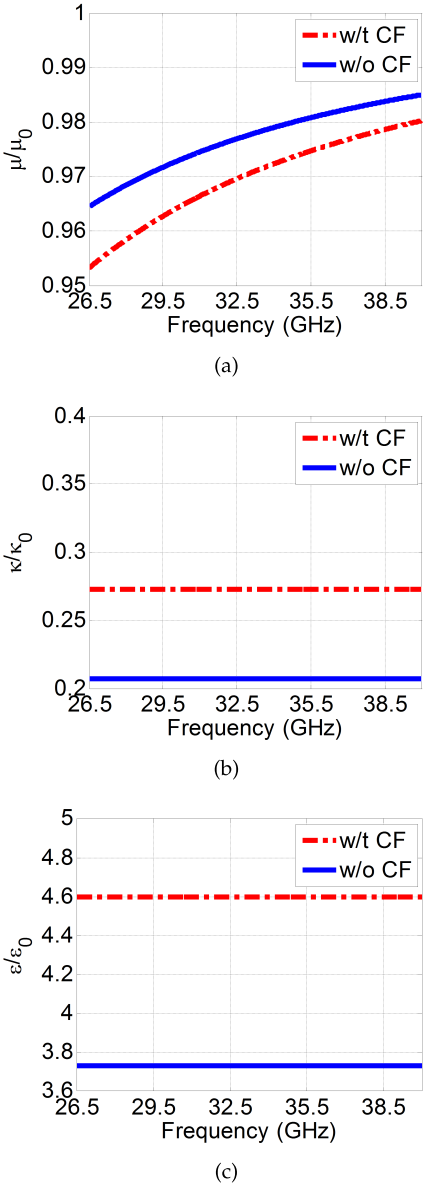

FIGURE 6. The effective model parameters in the case of WR-28 ($4\pi M_s = 6000$ G, $H_0 = 2400$ Oe, $\frac{\Delta S}{S} = 0.075$, $Fr_{asr} = 7$). (a) $\frac{\mu}{\mu_0}$. (b) $\frac{\kappa}{\kappa_0}$. (c) $\frac{\epsilon}{\epsilon_0}$.

value for the correction factor with respect to frequency (it is not a frequency dependent value). As the equations (34) through (37) show, this factor depends only on the physical dimensions of the ferrite slab and the dimensions of the rectangular waveguide cross-section. Hence, the proposed model along with this correction factor can obtain the phase shift in all rectangular waveguide standards loaded with horizontal ferrite slabs with slight deviation as will be discussed in Section V.

Some examples are selected to show the effect of the CF on Equations (4), (5), and (6). The CF is function of the $\frac{\Delta S}{S}$ and Fr_{asr} as shown before. Thus, the three standard waveguides WR-650, WR-90, and WR-28 are selected, each of them has a $\frac{\Delta S}{S} = 0.075$, and $Fr_{asr} = 7$. Nevertheless, other filling factors and aspect ratios are valid, only those examples are selected to facilitate the article readability. The effective model parameters with and without the correction factor for the selected examples are shown in Fig 4, Fig. 5, and Fig. 6.

V. VALIDATION AND EXPERIMENTAL RESULTS

Many cases using different standard waveguides have been studied and investigated to validate the proposed inhomogeneous model equations. Some cases have been selected and presented in this section. The selected waveguides are WR-650, WR-90, and WR-28 that covers the L-band, X-band, and Ka-band, respectively. Each case is evaluated using the proposed inhomogeneous model equations and then compared with both of the approximate relation and the

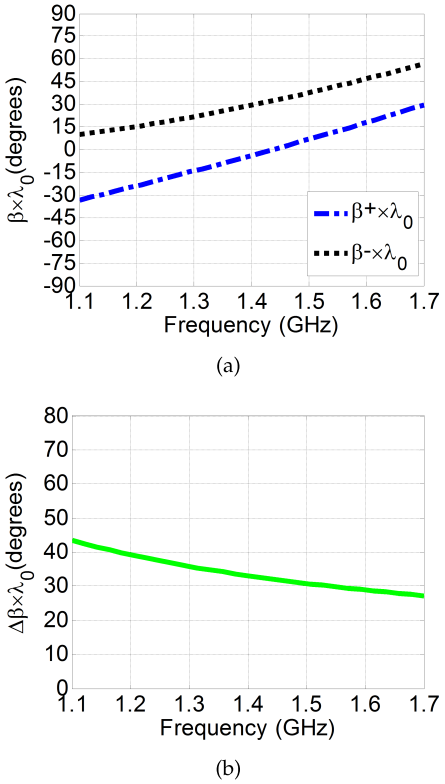

FIGURE 7. $\beta \times \lambda_0$ components for WR-650 ($4\pi M_s = 300$ G, $H_0 = 120$ Oe, $\frac{\Delta S}{S} = 0.075$, $Fr_{asr} = 7$). (a) $\beta + \times\lambda_0$ and $\beta - \times\lambda_0$. (b) $\Delta\beta \times \lambda_0$.

numerical simulation results. Suitable parameters are selected for each case. The differential phase ($\Delta\beta$) for each case is calculated for a guided wavelength at the center frequency (λ_0)of each corresponding band.

The comparison of the three methods for the standard waveguide WR-650 is shown in Fig. 8, the behavior of the three curves is almost the same with slight deviations for the small filling factor ($\frac{\Delta S}{S} = 0.01$), meanwhile, for larger filling factor ($\frac{\Delta S}{S} = 0.075$) the proposed model is very close to the numerical simulation results with the deviation that does not exceed 10%. The same behavior for the other standard waveguides WR-90 and WR-28, their comparisons are shown in Figs. 9, and 10, respectively. It is clear from the shown comparison curves that the approximate relation has an acceptable percentage error for small ferrite filling factors but not for the high filling factors. On the other side, the proposed model finds a value of the differential phase that is much closer to the true one. The error percentage of the proposed model as a function of $\frac{\Delta S}{S}$ and Fr_{asr} is plotted and shown in Fig. 11.

The approximate relation is based on oversimplifying the phase shift expressions of the vertical slab while using this expression in all cases [33]. As a result, this relation fails to obtain the phase shift with reasonable accuracy in many cases, especially in the case of the horizontal slab. On the other hand, the proposed model defines an effective region with a correction factor for the slab height to model the ferrite loaded rectangular waveguide (as described before).

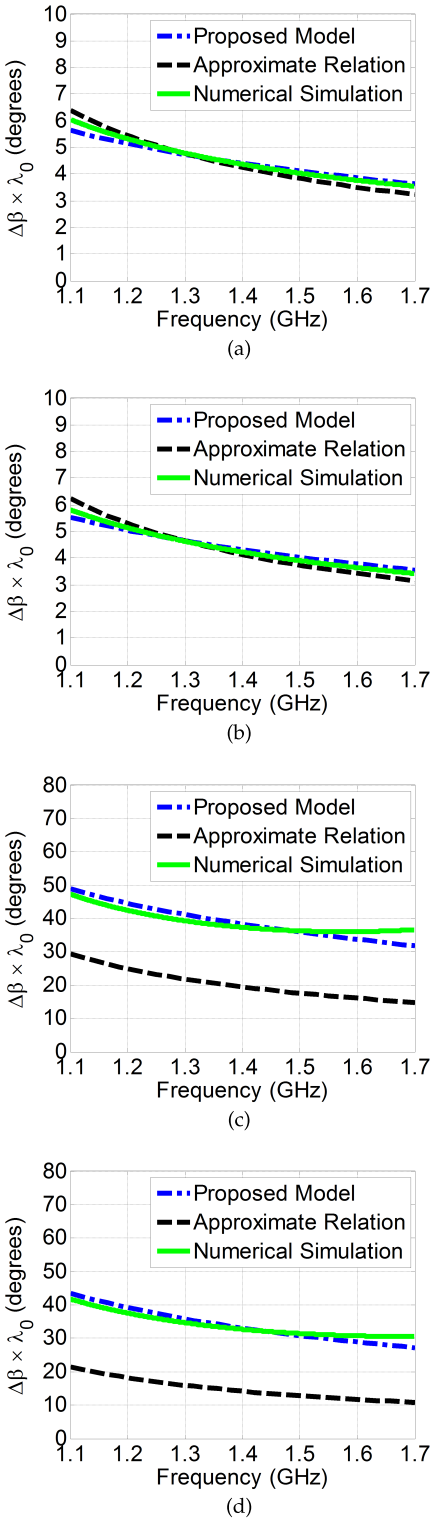

FIGURE 8. Comparing proposed inhomogeneous. model with CST and Approx. model (WR-650, $4\pi M_s = 300$ G, $H_0 = 120$ Oe). (a) $\frac{\Delta S}{S} = 0.01$, $Fr_{asr} = 5$. (b) $\frac{\Delta S}{S} = 0.01$, $Fr_{asr} = 7$. (c) $\frac{\Delta S}{S} = 0.075$, $Fr_{asr} = 5$. (d) $\frac{\Delta S}{S} = 0.075$, $Fr_{asr} = 7$.

This model can obtain the phase shift with a reasonable accuracy as shown in Figs. 8, 9, and 10, where the proposed correction factor is a part of the presented model.

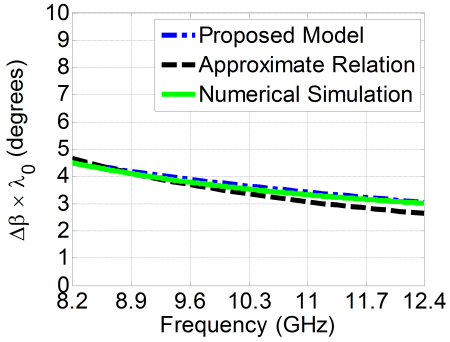

(a)

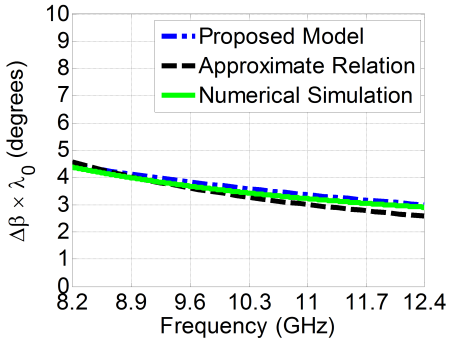

(b)

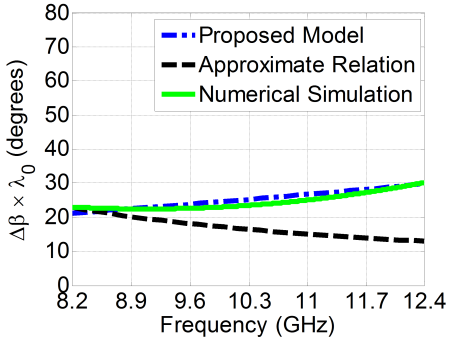

(c)

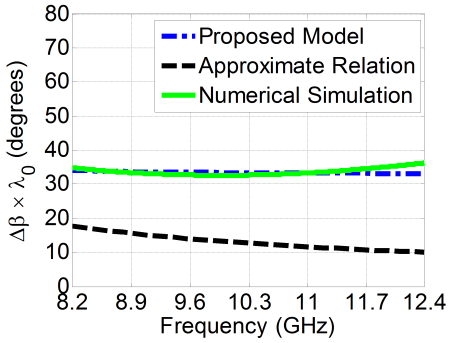

(d)

FIGURE 9. Comparing proposed inhomogeneous. model with CST and Approx. model (WR-90, $4\pi M_s = 1880$ G, $H_0 = 752$ Oe).
(a) $\frac{\Delta S}{S} = 0.01$, $Fr_{asr} = 5$. (b) $\frac{\Delta S}{S} = 0.01$, $Fr_{asr} = 7$.
(c) $\frac{\Delta S}{S} = 0.075$, $Fr_{asr} = 5$. (d) $\frac{\Delta S}{S} = 0.075$, $Fr_{asr} = 7$.

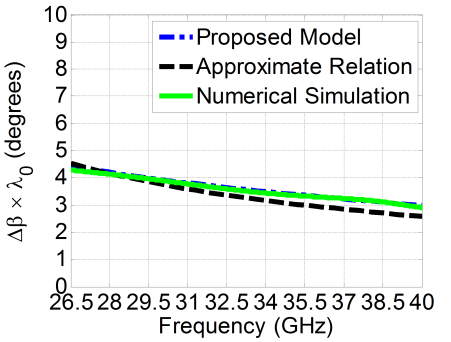

(a)

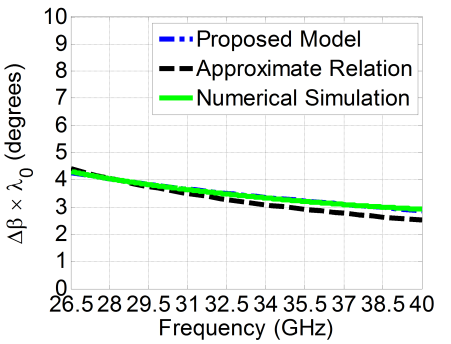

(b)

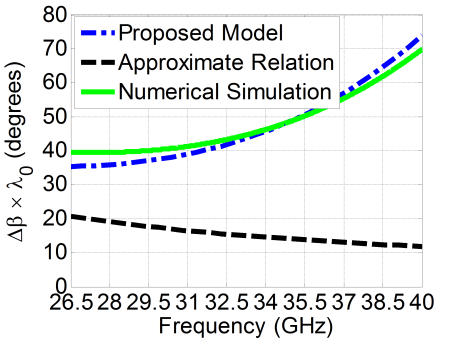

(c)

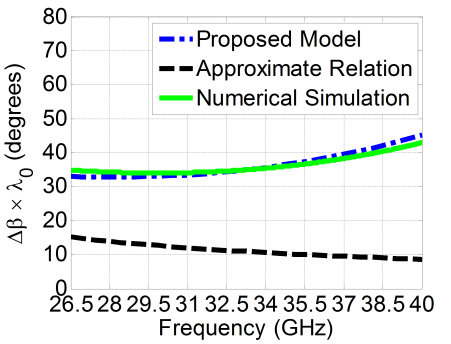

(d)

FIGURE 10. Comparing proposed inhomogeneous. model with CST and Approx. model (WR-28, $4\pi M_s = 6000$ G, $H_0 = 2400$ Oe).
(a) $\frac{\Delta S}{S} = 0.01$, $Fr_{asr} = 5$. (b) $\frac{\Delta S}{S} = 0.01$, $Fr_{asr} = 7$.
(c) $\frac{\Delta S}{S} = 0.075$, $Fr_{asr} = 5$. (d) $\frac{\Delta S}{S} = 0.075$, $Fr_{asr} = 7$.

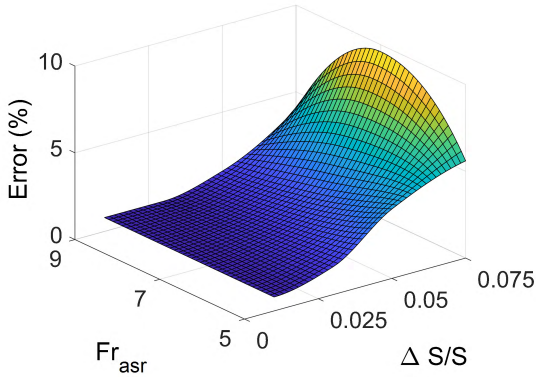

FIGURE 11. Proposed inhomogeneous model percentage error as a function of $\frac{\Delta S}{S}$ and Fr_{asr}.

The approximate model is very close as long as the filling factor is extremely small (below 1%). Thus, we proposed our model to cover both small and large values for filling factors, which is needed for practical applications. Our model is valid up to 0.075 filling factor (7.5%), which can cover all the practical applications of these components. Nevertheless, our model is valid for all frequency bands.

The deviation between the proposed model and the numerical solution is limited as the error calculated in all standard waveguide is below 10%, which can be depicted from Fig. 11. However, this can be enhanced by calculating an effective ferrite slab width to the ferrite slab to take into consideration the fringing fields as an future extension to this work.

An example is constructed and measured in favor of comparing it with the proposed model as well as the simulations. This example utilizes the standard waveguide WR-28 with two ferrite slabs per channel as described before. The ferrite material is nickel ferrite with zinc substitution with $4\pi M_s = 5300$ G, $\epsilon_r = 13.5$, and $\tan\delta = 0.0006$. Each ferrite slab has dimensions of $25.4 \times 1.9 \times 0.56\ mm^3$. Thus the ferrite filling factor $\frac{\Delta S}{S}$ is 0.084 and each slab aspect ratio Fr_{asr} is 3.4. The frequency range of the comparison between measurements and other methods (proposed model, approximate relation, and numerical simulation) is limited to 26.5-34 GHz due to limitations of the fabrication with respect to the exact values of dimensions and $4\pi M_s$.

The setup of the fabricated example consists of one channel in order to facilitate the setup. This is equivalent to the differential phase shift between two channels that have the same ferrite slabs with the same direction and magnitude of magnetization. The only difference between the two channels is the ferrite slabs location; each channel is a mirrored version of the other. The measurement setup is shown in Fig. 12(a). The comparisons of the measured differential phase shift, and the S-parameters magnitudes simulation and measurement comparison are shown in Fig. 12.

It is clear from Fig. 12(b) that the approximate relation fails at higher frequencies, meanwhile, the proposed model is very close to the simulations. In this figure, we tried three tolerance values (±5%, ±7.5%, and ±10%). The closest curve to the

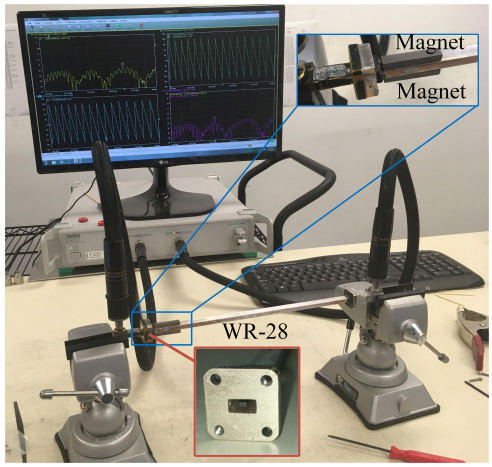

(a)

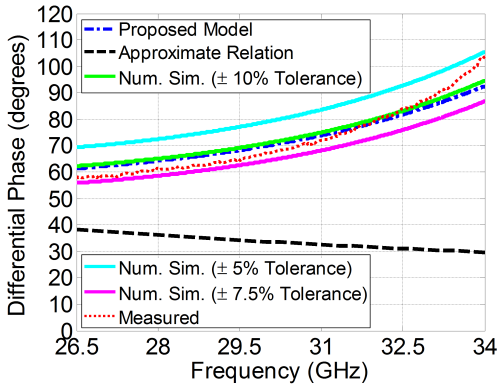

(b)

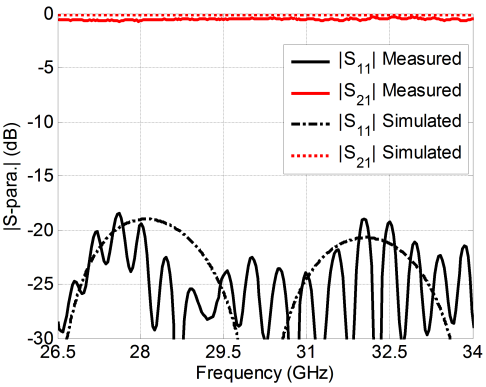

(c)

FIGURE 12. Fabricated example. (a) Measurement setup. (b) Measured differential phase shift comparison with simulations, approximate model, and proposed model. (c) S-parameters magnitudes simulation and measurement comparison.

measurements is the one with ±10% tolerance as shown in Fig. 12(b). The other two curves indicate a significant deviation. The reason for such a deviation between the measured and simulated phase can be attributed to the tolerance of the ferrite slabs alignment, which was difficult to verify due to the long and narrow closed waveguide. In addition, the value of H_0 of the magnet is tough to achieve practically with a precise

value. Nevertheless, the magnitude of the $4\pi M_s$ of the ferrite material has $\pm 5\%$ tolerance, and its physical parameters are measured at 9 GHz by the manufacturer. Those physical parameters can change a bit at the 30 GHz band. Thus, some deviations in the measurements are expected. In Fig. 12(c) the matching level is acceptable. However, these ripples are attributed to the effect of the ferrite slabs and the magnets. Moreover, the insertion loss levels of the measurements and the simulations are close to each other.

VI. CONCLUSIONS

A full study of the non-reciprocal ferrite based differential phased shifters has been presented showing the main criteria of the material selection and the traditional methodology for designing such shifters. Also, the limitations of this methodology are discussed. Moreover, a homogeneous solution with modeled equations to determine the differential phase occurring in such phase shifters has been proposed. Nevertheless, a novel inhomogeneous model with accurate equations is proposed for such shifters. Later, many cases are studied to validate the proposed modeled equations that have a very good agreement with simulations with a maximum error does not exceed 10%. In conclusion, an accurate model is proposed and validated to obtain the phase shift for the ferrite loaded rectangular waveguide. This structure is an essential building block in duplexers, which are deployed in all radar systems till now. Finally, an example has been selected for prototyping, and then the measured results are compared with the proposed model, the approximate relation, and the numerical simulation. The measurements of the differential phase shift, insertion loss, and matching have accepted values and levels that validate the proposed model.

APPENDIX
FERRITE MATERIAL SELECTION CRITERIA

Designing differential phase shifters based on ferrite materials need many considerations to assure that the selected ferrite material will perform the required operation. Selection of such materials depends mainly on basic parameters such as the saturation magnetization factor ($4\pi M_s$), magnetic DC bias (H_0), Larmor frequency (f_0), and the saturated magnetic frequency (f_m). These parameters are related to each other, and these relations are shown in the following equations [33].

$$f_0(MHz) = 2.8 \times H_0(Oe) \tag{38}$$

$$f_m(MHz) = 2.8 \times 4\pi M_s(G) \tag{39}$$

The criteria for selecting the ferrite material must consider the following notes:

- The ferrite must be at least saturated. However, it is always recommended to operate above saturation. This ensures that some slight deterioration of the magnets will not lead to lose the saturation of the ferrite
- The operating frequency band of the differential phase shifter must be outside the resonance frequency band of the ferrite, this means the prohibited band is between $\sqrt{f_0 \times (f_0 + f_m)}$ and $f_0 + f_m$ [43].

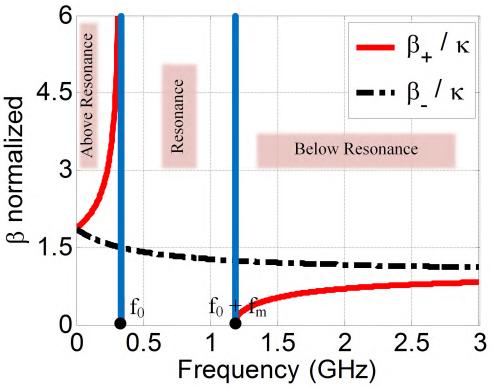

FIGURE 13. Normalized phase constant vs frequency of ferrite sample ($4\pi M_s = 300$ G, and $H_0 = 120$ Oe).

- The operating band can be above resonance (i.e. $< \sqrt{f_0 \times (f_0 + f_m)}$) or below resonance (i.e. $> f_0 + f_m$).
- In the below resonance band as the frequency increases the differential phase decreases till it reaches almost zero at very high frequencies. That means, in order to have a reasonable phase shift, the upper frequency of the operating band of the differential phase shifter must be at least around $1.1 \times (f_0 + f_m)$ or slightly higher.

An example of the phase constant versus frequency in the ferrite medium case is illustrated in Fig. 13. The phase constant β inside the ferrite material can be defined by the following equation:

$$\beta_{\pm}/\kappa = \omega\sqrt{(\mu \pm \kappa)/\mu_0} \tag{40}$$

β_+ and β_- corresponds to the RHCP and LHCP waves, respectively. Fig. 13 also shows the three bands of operation; above resonance, resonance, and below resonance.

As a summary, the key factors to select the suitable ferrite material are the saturation magnetization factor and the magnetic DC bias, which subsequently determine the values of Larmor frequency and saturated magnetic frequency.

REFERENCES

[1] W. Tatinian and J. Lanteri, "Electronical beam scanning using integrated CMOS continuous $0° - 360°$ phase shifter," in *Proc. IEEE Conf. Antenna Meas. Appl. (CAMA)*, Nov. 2014, pp. 1–4.
[2] S. I. Shams, M. A. Abdelaal, and A. A. Kishk, "Broadside uniform leaky-wave slot array fed by ridge gap splitted line," in *Proc. IEEE Int. Symp. Antennas Propag. USNC/URSI Nat. Radio Sci. Meeting*, Jul. 2015, pp. 2467–2468.
[3] S. I. Shams, M. A. Abdelaal, and A. A. Kishk, "SIW magic tee fed by printed ridge gap waveguide design," in *Proc. 17th Int. Symp. Antenna Technol. Appl. Electromagn. (ANTEM)*, Jul. 2016, pp. 1–2.
[4] M. A. Abdelaal and A. A. Kishk, "Circularly polarized dielectric resonator antenna for UMTS and WLAN applications," in *Proc. USNC-URSI Radio Sci. Meeting (Joint AP-S Symp.)*, Jul. 2015, p. 335.
[5] X. Hong, Y. Xia, B. Muneer, and Z. Qi, "Design of polarization-agile antenna by using integrated structure of phase shifter and power divider," in *Proc. IEEE 4th Asia–Pacific Conf. Antennas Propag. (APCAP)*, Jun./Jul. 2015, pp. 523–524.
[6] M. A. Abdelaal and A. A. Kishk, "Wideband circularly polarized dielectric resonator antenna for GPS and GNSS applications," in *Proc. 17th Int. Symp. Antenna Technol. Appl. Electromagn. (ANTEM)*, Jul. 2016, pp. 1–2.

[7] M. A. Abdelaal, S. I. Shams, and A. A. Kishk, "Asymmetric compact OMT for X-band SAR applications," *IEEE Trans. Microw. Theory Techn.*, vol. 66, no. 4, pp. 1856–1863, Apr. 2018.
[8] M. A. Abdelaal, S. I. Shams, M. A. Moharram, M. Elsaadany, and A. A. Kishk, "Compact full band OMT based on dual-mode double-ridge waveguide," *IEEE Trans. Microw. Theory Techn.*, vol. 66, no. 6, pp. 2767–2774, Jun. 2018.
[9] J. Russat, J.-P. Nicolai, P. Morvan, and N. Fel, "A delay line phase shifter for ultrawide-band operation," in *Proc. 28th Eur. Microw. Conf.*, vol. 2, Oct. 1998, pp. 669–672.
[10] S. Lucyszyn and I. D. Robertson, "Decade bandwidth hybrid analogue phase shifter using MMIC reflection terminations," *Electron. Lett.*, vol. 28, no. 11, pp. 1064–1065, May 1992.
[11] X. Tang and K. Mouthaan, "Design of large bandwidth phase shifters using common mode all-pass networks," *IEEE Microw. Wireless Compon. Lett.*, vol. 22, no. 2, pp. 55–57, Feb. 2012.
[12] D. Adler and R. Popovich, "Broadband switched-bit phase shifter using all-pass networks," in *IEEE MTT-S Int. Microw. Symp. Dig.*, vol. 1, Jul. 1991, pp. 265–268.
[13] S. J. Kim and N. H. Myung, "A new active phase shifter using a vector sum method," *IEEE Microw. Guided Wave Lett.*, vol. 10, no. 6, pp. 233–235, Jun. 2000.
[14] B.-W. Min and G. M. Rebeiz, "Ka-band BiCMOS 4-bit phase shifter with integrated LNA for phased array T/R modules," in *IEEE MTT-S Int. Microw. Symp. Dig.*, Jun. 2007, pp. 479–482.
[15] M. Meghdadi, M. Azizi, M. Kiani, A. Medi, and M. Atarodi, "A 6-bit CMOS phase shifter for S-band," *IEEE Trans. Microw. Theory Techn.*, vol. 58, no. 12, pp. 3519–3526, Dec. 2010.
[16] D. W. Kang and S. Hong, "A 4-bit CMOS phase shifter using distributed active switches," *IEEE Trans. Microw. Theory Techn.*, vol. 55, no. 7, pp. 1476–1483, Jul. 2007.
[17] J. W. Simon, "Broadband strip-transmission line Y-junction circulators," *IEEE Trans. Microw. Theory Techn.*, vol. MTT-13, no. 3, pp. 335–345, May 1965.
[18] A. Clavin, "High-power ferrite load isolators," *IRE Trans. Microw. Theory Techn.*, vol. 3, no. 5, pp. 38–43, Oct. 1955.
[19] F. Reggia and E. G. Spencer, "A new technique in ferrite phase shifting for beam scanning of microwave antennas," *Proc. IRE*, vol. 45, no. 11, pp. 1510–1517, Nov. 1957.
[20] H. Scharfman, "Three new ferrite phase shifters," *Proc. IRE*, vol. 44, no. 10, pp. 1456–1459, Oct. 1956.
[21] R. Babbitt and R. Stern, "Fabrication and performance of ferrite phase shifters for millimeter frequencies," *IEEE Trans. Magn.*, vol. MAG-15, no. 6, pp. 1744–1746, Nov. 1979.
[22] C. E. Fay and R. L. Comstock, "Operation of the ferrite junction circulator," *IEEE Trans. Microw. Theory Techn.*, vol. MTT-13, no. 1, pp. 15–27, Jan. 1965.
[23] Y. Konishi and N. Hoshino, "Design of a new broad-band isolator," *IEEE Trans. Microw. Theory Techn.*, vol. MTT-19, no. 3, pp. 260–269, Mar. 1971.
[24] C. E. Fay, "Ferrite switches in coaxial or strip transmission line," in *PGMTT Nat. Symp. Dig.*, Washington, DC, USA, 1962, pp. 119–125. [Online]. Available: http://ieeexplore.ieee.org/stamp/stamp.jsp?tp=&arnumber=1122398&isnumber=24823. doi: 10.1109/PGMTT.1962.1122398.
[25] C. R. Boyd, "A dual-mode latching reciprocal ferrite phase shifter," *IEEE Trans. Microw. Theory Techn.*, vol. MTT-18, no. 12, pp. 1119–1124, Dec. 1970.
[26] J. Vinding, "Ferrite switches in radar duplexers," in *Proc. WESCON/57 Conf. Rec.*, vol. 1, Aug. 1957, pp. 71–76.
[27] B. Lax, K. J. Button, and L. M. Roth, "Ferrite phase shifters in rectangular wave guide," *J. Appl. Phys.*, vol. 25, no. 11, pp. 1413–1421, 1954.
[28] S. Weisbaum and H. Boyet, "Broad-band nonreciprocal phase shifts—Analysis of two ferrite slabs in rectangular guide," *J. Appl. Phys.*, vol. 27, no. 5, pp. 519–524, 1956.
[29] M. L. Kales, H. N. Chait, and N. G. Sakiotis, "A nonreciprocal microwave component," *J. Appl. Phys.*, vol. 24, no. 6, pp. 816–817, 1953.
[30] A. G. Fox, S. E. Miller, and M. T. Weiss, "Behavior and applications of ferrites in the microwave region," *Bell Syst. Tech. J.*, vol. 34, no. 1, pp. 5–103, Jan. 1955.
[31] B. Lax, "Frequency and loss characteristics of microwave ferrite devices," *Proc. IRE*, vol. 44, no. 10, pp. 1368–1386, Oct. 1956.
[32] B. Lax and K. J. Button, *Microwave Ferrites and Ferrimagnetics*. New York, NY, USA: McGraw-Hill, 1962.
[33] D. M. Pozar, *Microwave Engineering*, 4th ed. Hoboken, NJ, USA: Wiley, 2011.
[34] C. E. Fay, "Ferrite-tuned resonant cavities," *Proc. IRE*, vol. 44, no. 10, pp. 1446–1449, Oct. 1956.
[35] A. Clavin, "Reciprocal ferrite phase shifters in rectangular waveguide (correspondence)," *IRE Trans. Microw. Theory Techn.*, vol. 6, no. 3, p. 334, Jul. 1958.
[36] G. J. Buck, "Ferrite microstrip phase shifters-theory and experiment," in *Proc. G-MTT Int. Microw. Symp.*, May 1970, pp. 332–336,
[37] M. E. Hines, "Ferrite phase shifters and multi-port circulators in microstrip and stripline," in *IEEE GMTT Int. Microw. Symp. Dig.*, May 1971, pp. 108–109.
[38] F. A. Ghaffar and A. Shamim, "Theory and design of a half-mode SIW ferrite LTCC phase shifter," in *IEEE MTT-S Int. Microw. Symp. Dig.*, May 2015, pp. 1–3.
[39] M. A. Abdelaal, S. I. Shams, and A. A. Kishk, "90 ° phase shifter based on substrate integrated waveguide technology for Ku-band applications," in *Proc. 31st Ind. Gen. Assem. Sci. Symp. Int. Union Radio Sci. (URSI GASS)*, Aug. 2017, pp. 1–3.
[40] M. A. Abdelaal, S. I. Shams, and A. A. Kishk, "Compact RGW differential phase shifter for millimeter-wave applications," in *Proc. 18th Int. Symp. Antenna Technol. Appl. Electromagn. (ANTEM)*, Aug. 2018, pp. 1–2.
[41] M. A. Abdelaal, S. I. Shams, and A. A. Kishk, "Circularly polarized RGW slot antenna fed by ferrite based phase shifter," in *Proc. 18th Int. Symp. Antenna Technol. Appl. Electromagn. (ANTEM)*, Aug. 2018, pp. 1–2.
[42] J. R. Bray and L. Roy, "Development of a millimeter-wave ferrite-filled antisymmetrically biased rectangular waveguide phase shifter embedded in low-temperature cofired ceramic," *IEEE Trans. Microw. Theory Techn.*, vol. 52, no. 7, pp. 1732–1739, Jul. 2004.
[43] M. F. Farooqui, A. Nafe, and A. Shamim, "Inkjet printed ferrite-filled rectangular waveguide X-band isolator," in *IEEE MTT-S Int. Microw. Symp. Dig.*, Jun. 2014, pp. 1–4.

MOHAMED A. ABDELAAL (S'12) received the B.Sc. (Hons.) degree from Modern Academy, Faculty of Engineering, Electronics and Communications Technology Department, Cairo, Egypt, in 2008, and the M.Sc. degree from the Arab Academy for Science, Technology & Maritime Transport, Faculty of Engineering, Electronics and Communications Department, Cairo, in 2013. He is currently pursuing the Ph.D. degree with the Electrical and Computer Engineering Department, Concordia University, Montreal, QC, Canada.

From 2008 to 2014, he served as a Teaching and Research Assistant with the Department of Electronics and Communications Technology, Faculty of Engineering, Modern Academy, Cairo, Egypt. From 2009 to 2013, he served as a Teaching and Research Assistant with the Department of Electronics and Communications, Faculty of Engineering, Arab Academy for Science, Technology & Maritime Transport, Cairo. Since 2014, he has been a Research Assistant with Concordia University. His research interests include orthomode transducers design and analysis, microwave reciprocal/nonreciprocal devices design and analysis, ferrite materials-based microwave devices design and analysis, dielectric resonators antenna design, millimeter wave antennas and devices, antenna design, and ridge gap waveguide technology.

He was ranked the first over 600 students in the bachelor's degree achieving a grade of 95.92 %. He received Concordia University International Tuition Fee Remission Award and Graduate Student Support Program Award in 2014 for his excellence. Also, he received the Canadian National Committee-International Union of Radio Science (CNC-URSI) Student Travel Award in 2015. He has served as a Reviewer for *The Institute of Engineering and Technology (IET) Journal*.

SHOUKRY I. SHAMS (S'04–M'17) received the B.Sc. (Hons.) and M.Sc. degrees in electronics and communications engineering from Cairo University, Egypt, in 2004 and 2009, respectively, and the Ph.D. degree in electrical and computer engineering from Concordia University, Montreal, QC, Canada, in 2016.

From 2005 to 2006, he served as a Teaching and Research Assistant with the Department of Electronics and Communications Engineering, Cairo University. From 2006 to 2012, he served as a Teaching and Research Assistant with the IET Department, German University in Cairo. From 2012 to 2016, he was a Teaching and Research Assistant with Concordia University. His research interests include microwave reciprocal/nonreciprocal design and analysis, high power microwave subsystems, antenna design, and material measurement.

Dr. Shams received the Faculty Certificate of Honor in 1999, The Distinction with Honor in 2004 from Cairo University. He received the Concordia University Recruitment Award in 2012 and Concordia University Accelerator Award in 2016. He was the GUC-IEEE Student Branch Chair from 2010 to 2012.

AHMED A. KISHK (S'84–M'86–SM'90–F'98) received the B.S. degree in electronic and communication engineering from Cairo University, Cairo, Egypt, in 1977, the B.Sc. degree in applied mathematics from Ain Shams University, Cairo, Egypt, in 1980, and the M. Eng. and Ph.D. degrees from the University of Manitoba, Winnipeg, Canada, in 1983 and 1986, respectively, where he joined the Department of Electrical Engineering in 1981. He was a Professor with the University of Mississippi from 1995 to 2011. He has been a Professor with Concordia University, Montreal, QC, Canada, since 2011, as a Tier 1 Canada Research Chair in advanced antenna systems.

He has published more than 320-refereed Journal articles and 450 conference papers. He has several patents to his credit. He has co-authored four books and several book chapters and the editor of three books. He offered several short courses in international conferences. His research interests include millimeter wave antennas for 5G applications, analog beamforming networks, dielectric resonator antennas, microstrip antennas, small antennas, microwave sensors, RFID antennas for readers and tags, multi-function antennas, microwave circuits, EBG, artificial magnetic conductors, soft and hard surfaces, phased array antennas, reflect/transmitarray, wearable antennas, and feeds for parabolic reflectors.

Dr. Kishk and his students were the recipients of several awards. For example, he received the Microwave Theory and Techniques Society, Microwave Prize 2004 and 2013 Chen-To Tai Distinguished Educator Award of the IEEE Antennas and Propagation Society. In recognition for contributions and continuous improvements to teaching and research to prepare students for future careers in antennas and microwave circuits. He was a Feature articles Editor of *Antennas & Propagation Magazine* from 1993 to 2014. He was an Editor-in-Chief of the ACES Journal from 1998 to 2001. He was a member of the AP AdCom from 2013 to 2015 and the 2017 AP-S President.